Histol Histopathol (2020) 35: 1295-1307

http://www.hh.um.es

Histology and Histopathology
From Cell Biology to Tissue Engineering

An association between successful engraftment of osteosarcoma patient-derived xenografts and clinicopathological findings

Anneliese Fortuna-Costa[1]*, Regina Alcantara Granato[2]*, Walter Meohas[3], Ana Cristina de Sá Lopes[3], Anabela Cunha Caruso[1], Rafael Castro e Silva Pinheiro[3], Pedro da Gama d'Eça[3], Rhayra Braga Dias[1], Jamila Alessandra Perini[1], Ana Paula Fernandes Barbosa[4], Renato Augusto Moreira de Sá[5], João Antonio Matheus Guimarães[1], Samuel S. Murray[6] and Maria Eugenia Leite Duarte[1]

[1]Research Division, National Institute of Orthopedics and Traumatology (INTO), Rio de Janeiro, RJ, Brazil, [2]Department of Pathology, Federal Fluminense University, Niterói, RJ, Brazil, [3]Center of Orthopedic Oncology, National Institute of Orthopedics and Traumatology (INTO), Rio de Janeiro, RJ, Brazil, [4]Department of Pathology, Federal University of Alagoas, Maceió, AL, Brazil, [5]Department of Internal Medicine, Federal Fluminense University, Niterói, RJ, Brazil and [6]Department of Medicine, University of California, Los Angeles and VA Greater Los Angeles Healthcare System, Los Angeles, CA, USA

*These authors contributed equally to this work

Summary. Although osteosarcoma is a rare disease, with a global incidence rate estimated at 5.0/million/year, it is the most frequent primary bone sarcoma in children and adolescents. In translational research, the patient-derived xenograft (PDX) model is considered an authentic *in vivo* model for several types of cancer, as tumorgrafts faithfully retain the biological characteristics of the primary tumors. Our goal was to investigate the association between PDX formation and clinical findings of osteosarcoma patients and the ability of the model to preserve in immunocompromised mice the characteristics of the parental tumor. A fresh sample of the patient tumor obtained from a representative biopsy or from surgical resection was implanted into nude mice. When tumor outgrowths reached ~1,500 mm^3, fresh PDX fragments were re-transplanted into new hosts. Engraftment in mice was obtained after a latency period of 19-225 days (median 92 days) in 40.54% of the implanted samples. We confirmed the histopathological fidelity between the patient tumor and their respective established PDXs, including the expression of biomarkers. PDX take rate was higher in surgical resection samples, in post-chemotherapy surgical samples and in samples from patients with metastatic disease at presentation. In conclusion, we have shown that the osteosarcoma PDX model reliably recapitulates the morphological aspects of the human disease after serial passage in mice. The observation that more aggressive forms of osteosarcoma, including those with metastatic disease at presentation, have a higher efficiency to generate PDXs provides a promising scenario to address several unanswered issues in clinical oncology.

Key words: Osteosarcoma, Sarcomas, Musculoskeletal malignancies, Bone tumor, Patient-derived xenograft

Offprint requests to: Maria Eugenia Leite Duarte, Avenida Brazil 500, São Cristóvão, Zip code: 20940-070, Rio de Janeiro, RJ, Brazil. e-mail: meugenia.into@gmail.com

DOI: 10.14670/HH-18-256

Introduction

Osteosarcoma is among the most frequently diagnosed bone malignancies in both pediatric and young adult patients (Mirabello et al., 2009a,b; Noone et al., 2018). However, it is a rare disorder with an estimated incidence of 3-5 per million in males and 2-4 per million in females (Mirabello et al., 2009a). In about 80% of all osteosarcoma patients, the primary site is the knee region (metaphyses of distal femur and proximal tibia) (Bielack et al., 2002). Patients usually have nonspecific clinical symptoms, the most common of which is pain and/or swelling of the involved region (Bielack and Bernstein, 2005). Standard therapy consists of preoperative (neoadjuvant) chemotherapy followed by

surgery and postoperative (adjuvant chemotherapy) (Isakoff et al., 2015). Despite significant improvements in recent decades with the advances in surgery and multiagent chemotherapy, the overall 10-year survival rate for non-metastatic patients with localized resectable tumors is approximately 64.4%. For those with metastatic disease at diagnosis, the prognosis is substantially poorer, with a ten-year survival rate of 26% (Bielack et al., 2002; Isakoff et al., 2015).

In translational research, several *in vivo* preclinical models of human tumors are available to examine the biology of cancer, including animal models induced by xenografting cell lines of fresh cancer tissue specimens into immunodeficient mice (Langdon, 2012). Among these, patient-derived xenograft (PDX) tumor models are reported as more reliable in a preclinical setting as they retain cell population heterogeneity as well as histological and molecular characteristics of the original tumor (Garber, 2009; Tentler et al., 2012). Indeed, PDXs are currently considered an authentic *in vivo* model for several types of cancer (Garber, 2009; Siolas and Hannon, 2013) including osteosarcomas (Bruheim et al., 2004; Kresse et al., 2012; Monsma et al., 2012; Stewart et al., 2017; Meohas et al., 2018) as they most closely resemble the primary lesion and potentially recapitulate human tumor biology, including the characteristics of the microenvironment. A number of studies have validated the contention that the molecular and morphological features are well maintained between the patient tumor and PDX of osteosarcoma (Kresse et al., 2012; Monsma et al., 2012; Stewart et al., 2017; Meohas et al., 2018; Nanni et al., 2019). The potential of patient-derived xenografts to accurately reproduce the original tumor biology supports the importance of the model for the development of novel therapeutic strategies and as predictors of clinical outcomes (Press et al., 2008; Daniel et al., 2009; Kim et al., 2009; Ding et al., 2010).

The kinetics of PDX growth, including the variability in take rate, may reflect aspects of the clinical evolution of osteosarcoma with prognostic and therapeutic response implications. Furthermore, for several cancers, PDX formation is an indicator of worse clinical outcomes (John et al., 2011; Joshua et al., 2012; McAuliffe et al., 2015). Hence, our goal was to investigate PDX formation and the corresponding clinical and pathological data and determine whether the features of the PDX correlated with clinical findings. We also examined the ability of the model to preserve, in the immunocompromised mouse, the histological characteristics of the parenteral tumor.

Materials and methods

Patient recruitment

Tumor tissue samples from patients with a presumptive diagnosis of a primary osteosarcoma were obtained from January 2017 to November 2019 at the time of biopsy or surgical resection at the National Institute of Traumatology and Orthopedics in Rio de Janeiro, Brazil. The closing date for the study was set to April 2020 regarding a date of tumor recurrence. Patients treated preoperatively with neoadjuvant chemotherapy were also included in the study. This study was reviewed and approved by the Institutional Review Board (IRB). All medical records and clinical samples were collected with informed consent from the patients. Parents or legal guardians provided the consent for minors.

Human tissue specimens

A fresh sample of the patient tumor was obtained from a biopsy or from the surgical specimen resulting from tumor resection or limb amputation/disarticulation. For tumor samples obtained from surgical resection, experienced pathologists collected the fragments from solid areas, avoiding areas of necrosis and hemorrhage. Except for small samples obtained by biopsies, all implanted tissue was screened by histological examination to ensure that they were representative of the primary tumor.

The samples were maintained in Dulbecco's Modified Eagle Medium (DMEM) at 4°C until implantation. A single 2x5 mm cylindrical fragment of tumor tissue obtained by fluoroscopy-guided needle biopsy represented samples from biopsies. Tumor samples were collected, handled and stored under sterile conditions.

Establishment of patient-derived xenograft

All mice were maintained and treated in accordance with the Health Guide for the Care and Use of Experimental Animals with approval from the National Institute of Traumatology and Orthopedics Animal Care and Use Committee (Protocol no 005/2017). During the entire experimental period, the animals were kept in a barrier facility in high efficiency particulate air (HEPA)-filtered racks under standard conditions of 12-hour light/dark cycles and were fed *ad libitum* with irradiated laboratory rodent diet and autoclaved water.

Establishment of osteosarcoma PDXs was performed as previously described (Meohas et al., 2018). Briefly, six to eight-week-old athymic nude mice (B6.Cg-*Foxn1*^{nu}) were anesthetized with isoflurane inhalation and, under sterile conditions, patient tumor samples were minced into small fragments (2-3 mm^3) and implanted (four/animal) into a subcutaneous area on the right and left flanks. All tumor samples used for transplantation were collected immediately following the surgical procedure and were implanted fresh in the mice within an average of 1 hour after patient's biopsy or main surgery procedures.

When tumor outgrowths reached ~1,500 mm^3 the mice were euthanized. Fresh PDX tumors were harvested, minced into 2-3 mm^3 fragments and were then re-transplanted into new hosts. The first established

PDX from the primary clinical sample was designated as passage 0 (P0) and subsequent passages were P1 and P2. Tumor growth was assessed by palpation and monitored weekly using a digital caliper. Tumor volume (TV) was calculated according to the formula: $TV=(ab^2)/2$, where, "a" is the length of the major axis of the tumor, and "b" is the length of its minor axis. The latency period for individual xenografts corresponded to the lag-time for the PDX outgrowth to reach a volume of ~200 mm^3. This time point was defined as the onset of tumor growth and the growth period (in days) was calculated as the total time required for tumors to reach the harvest thresholds (~1,500-2,000 mm^3). Growth failure was considered if PDX formation did not occur by seven months and the patient was scored as a "non-engrafter".

Histopathological characterization of xenografts

Once harvested, samples from all xenografted tumors were fixed in 4% buffered paraformaldehyde and embedded in paraffin blocks. Sections (3 μm thick) were stained with hematoxylin-eosin (H&E) and evaluated microscopically using Aperio ImageScope version 12.3.3 (Leica Biosystems Inc., Lincolnshire, IL, USA). Tissue sample slides were examined by experienced pathologists blinded for tumor passage to assess whether the histologic subtype of the patient's primary tumor was reproduced in the PDX tumor.

Immunohistochemistry

Representative sections of primary human tumors and PDXs were analyzed by immunohistochemistry for stability of expression of Ki-67, CD-31, and human lamin A/C. Immunohistochemistry was performed with Envision™ FLEX - HRP conjugated polymer kit (Dako, Glostrup, Denmark) according to the manufacturer's instructions. After deparaffinization and antigenic retrieval, specimens were labeled with antibodies against Ki-67 (clone MIB-1, Dako), CD-31 (clone JC70A, Dako) with reactivity to both mouse and human CD-31 or with anti-monoclonal lamin A/C (clone BEO-12, Boster Biological Technology, Pleasanton, CA, USA). Signal was developed with EnVision Flex Substrate Buffer incubation with diaminobenzidine (DAB) (Dako). Dako Antibody Diluent (Dako Agilent) was used as a substitute for the primary antibody in the negative control reaction. CD31 and Ki-67 expression patterns in the PDX outgrowths were compared with the tumor of origin.

Clinicopathological variables and engraftment rates

We assessed the association between positive engraftment of primary tumor samples and demographic as well as clinicopathological factors obtained for all patients either at the time of diagnosis or at the end of the study. The Enneking surgical staging for mesenchymal malignancies was also used in the comparison between engrafters and non-engrafters. The staging takes into account the clinical and radiographic features and classifies the neoplasm as stages I and II respectively, to low and high-grade lesions which are further divided into two subcategories (A, B) based on tumor containment in anatomic compartments (intracompartmental or extracompartmental). Stage III corresponds to any tumor with distant metastasis (Jawad and Scully, 2010).

Statistical analysis

All statistical analyses were performed with SPSS (Statistical Package for Social Sciences Inc., Chicago, IL, USA) program version 20.0 and statistical significance was set at $P<0.05$. Categorical variables were expressed as percentages and compared between groups with the Chi-square (χ^2) test or the Mann-Whitney test, when applicable. The Student's t test was used for comparison of quantitative variables. Age was expressed as the median and interquartile range (IQR). Associations between tumor engraftment and clinical features were analyzed using logistic regression with adjustment for potential confounders such as receipt of neoadjuvant chemotherapy, metastatic disease at the time of diagnosis, and the source of the tumor sample.

Results

Between 2017 and 2019, we implanted subcutaneously into immunodeficient mice fresh primary tissue samples from 44 patients with a presumptive diagnosis of osteosarcoma. The final diagnosis of osteosarcoma was histologically confirmed in 37 patients (24 male and 13 female) with a median age of 18 years (range, 6-47 years). Most tumors were located in the knee region (n=30, 81.08%), and the most common histological variant was central high-grade conventional osteosarcoma (n=31, 83.78%). Fifteen (40.54%) tumor samples successfully engrafted while 22 (59.45%) failed to form xenografts within 7 months. All 15 engrafted tumors showed full xenograft development up to the third passage on mice (Fig. 1).

The median time to tumor formation (latency period) after implantation of patient sample in mice was quite variable, ranging between 19 and 225 days, (median 92 days). The median growth period, defined by the time required for the xenografts to reach the size of 1,500-2,000 mm^3, was 172.5 days (range 52-367) for P0 (Fig. 2). No significant difference was observed in the median engraftment latency period between biopsy-derived or surgical resection-derived PDXs (92 days and 93.5 days, respectively). Likewise, there was no statistical difference between the median growth period of biopsy and surgical resection-derived PDXs (147 days and 204 days, respectively). To investigate metastatic spread, the lungs and livers from all mice were sampled at each transplant generation, and screened by histological examination. No metastases were detected either grossly

or by microscopic examination.

All fifteen-tumor graft derivatives of primary specimens showed remarkably similar morphology compared to the corresponding parental tumors, confirming biological consistency with the original tumor. Individual hallmark findings of the histological

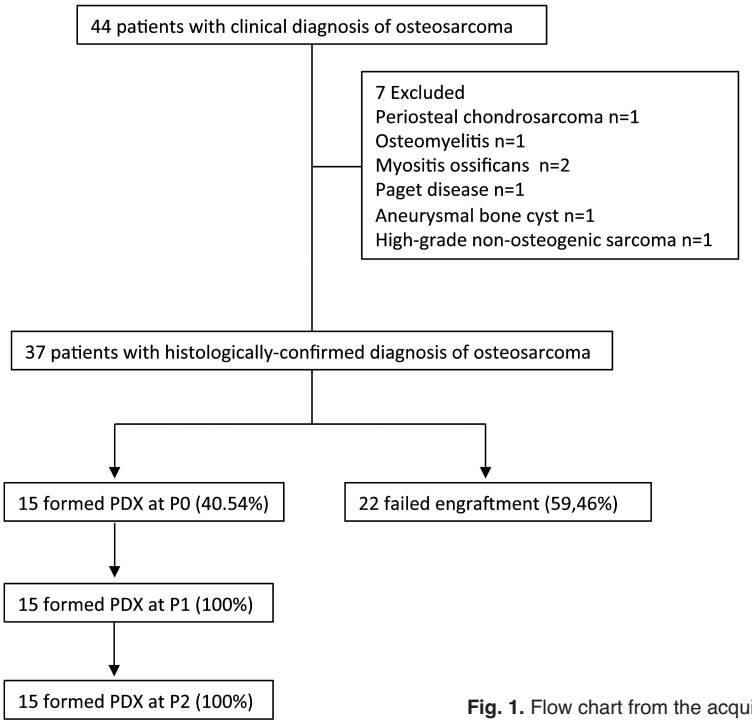


Fig. 1. Flow chart from the acquisition of osteosarcoma to tumor generation in athymic nude mice.

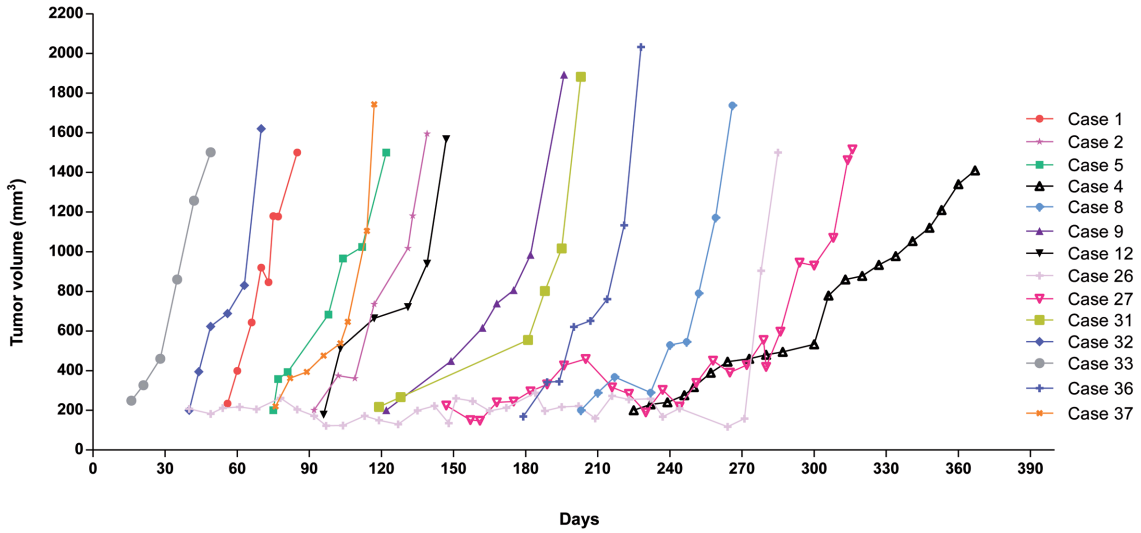


Fig. 2. Latency period and growth rates for PDX tumors grown in immunodeficient nude mice. Tumor size (mm^3) data were collected over time (days) for P0 in xenografts from OS patients. Samples of the patient tumor were obtained from a representative biopsy (cases 2, 4, 12, 32 and 37) or from surgical specimens (cases 1, 5, 7, 8, 9, 26, 27, 31, 33 and 36). The measurements of the PDX volume for case 7 were considered technically inaccurate and for this reason, are not displayed in the chart. The median latency period and growth period were 92 days (range 19-225) and 172.5 days (range 52-367), respectively. The median latency period for biopsy-derived PDXs was 92 days and for surgical resection-derived PDX was 92.5 days (p=0.742). The median growth period for PDXs derived from biopsies and surgical resection was 147 days and 204 days, respectively (p=0.899). Student's t-test.

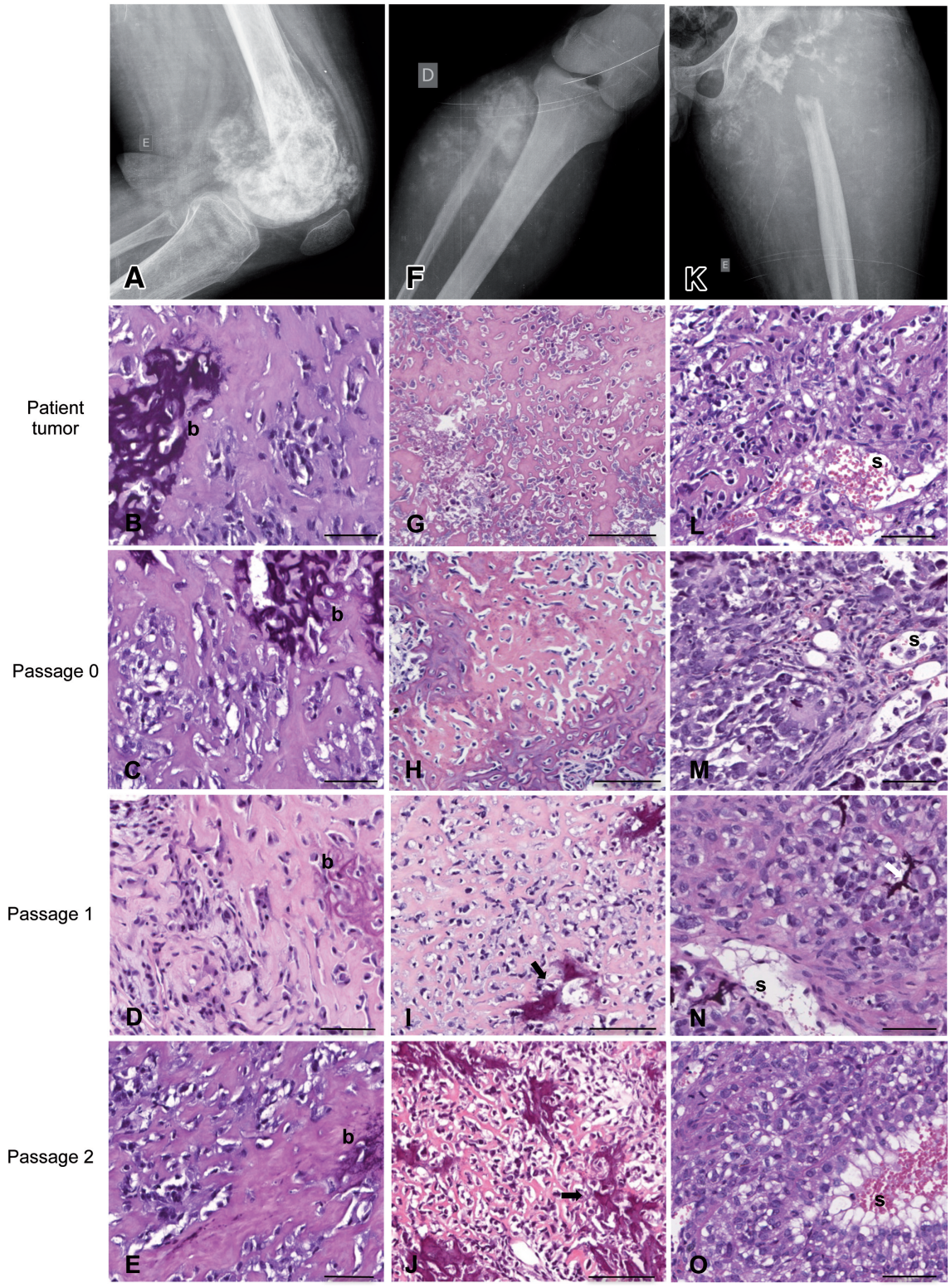


Fig. 3. Radiographic and histologic features from three representative patient-derived xenografts generated in athymic nude mice (B6.Cg-*Foxn1*^{nu}). The samples obtained from patient tumor demonstrate retained osteosarcoma histological subtypes in their matched PDX models up to passage 2. **A.** High-grade central osteosarcoma in a 14-year-old girl. The post-chemotherapy radiograph shows a large sclerotic lesion with irregular periosteal reaction involving the distal femur and surrounding soft tissue. **B.** Characteristic features of high-grade conventional central osteosarcoma such as the production of osteoid and bone matrix (b) into which the malignant cells are incorporate were retained in established PDXs at P0 **(C)**, P1 **(D)** and P2 **(E)** and are remarkably similar to the parental tumor **(B)**. **F.** High-grade central osteosarcoma in a 17-year-old boy. Plain radiograph of knee shows a large ill-defined lesion with cortical destruction involving the proximal fibula with soft tissue extension. **G.** Parental tumor represented by high-grade conventional central osteosarcoma featured by malignant osteoblasts with hyperchromatic nuclei surrounded by neoplastic bone. **H-J.** Histological features of high-grade osteosarcoma were maintained in established PDXs at all passages. **K.** Telangiectatic osteosarcoma in a 23-year-old man. Radiograph of the proximal femur reveals a lytic lesion with extensive bone destruction and expansion into soft tissue. **L.** Telangiectatic osteosarcoma featured by multiple blood-filled sinusoids (s), nuclear pleomorphism and a high mitotic rate in association with sparse bone matrix deposition were retained in all established PDXs **(M-O)**. H&E staining. Scale bars: B-E, 70 µm; G-J, 100 µm; L-O, 50 µm.

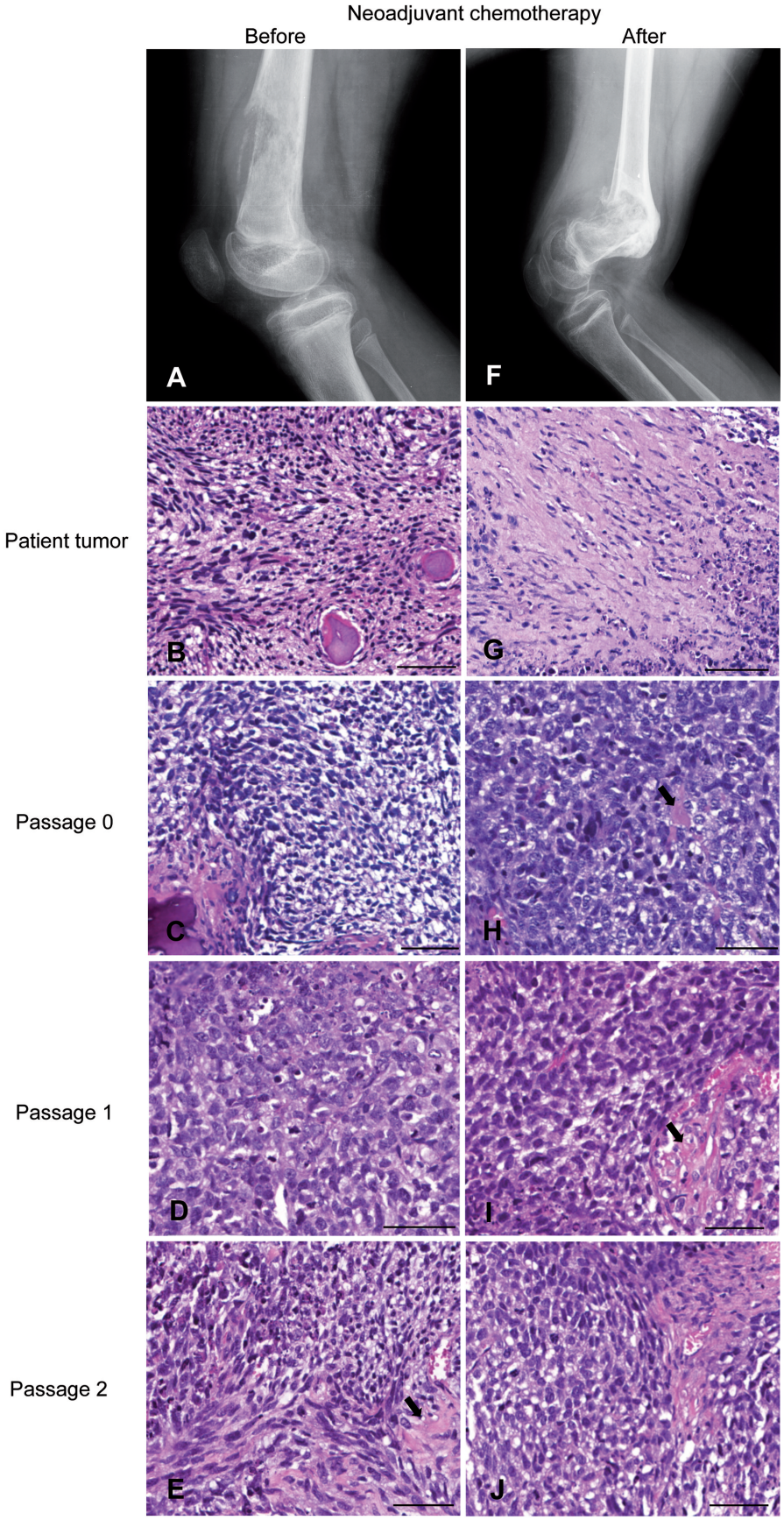


Fig. 4. Radiographic and histologic features from patient tumor and corresponding passages of the PDX models before and after neoadjuvant chemotherapy. **A.** Radiograph from an 11-year old boy with small cell osteosarcoma, showing a diffuse lytic/blastic lesion in the distal femur with a permeative pattern of the transition zone with cortical destruction and tumor expansion into soft tissue. **B.** Parental tumor diagnosis of small cell osteosarcoma featured by small cells with round, hyperchromatic nuclei and the production of scanty amounts of osteoid matrix was maintained in established PDXs at P0 **(C)**, P1 **(D)** and P2 **(E)**. **F.** Post-chemotherapy radiograph image reveals a central large sclerotic lesion with a pathologic fracture involving the distal femur. **G.** Small cell osteosarcoma showing alterations associated with a chemotherapy effect including viable tumor cells within a fibrotic stroma are depicted in the patient tumor sample. **H-J.** Histological features of small cell osteosarcoma were retained in representative tumor grafts at P0 **(H)**, P1 **(I)** and P2 **(J)** after neoadjuvant chemotherapy. Arrows: osteoid matrix. H&E staining. Scale bars: B-E, 70 µm; G, 100 µm.

osteosarcoma variants, including the production of neoplastic osteoid/bone matrix and nuclear pleomorphism were well retained between PDXs and the patient tumor (Fig. 3). One xenograft was found to grow as a blood-filled cystic mass at each transplant generation. The conservation of the original tumor microenvironment was confirmed by the presence of this bloody fluid, a distinctive feature of the primary parenteral telangiectatic osteosarcoma (Fig. 3L-O).

To investigate whether the components of the original tumor microenvironment were altered by the effect of chemotherapy, we established PDX models from a single patient before (Fig. 4A-E) and after chemotherapy treatment (Fig. 4F-J). The histological features characteristic of small cell osteosarcoma subtype, including hyperchromatic nuclei and the production of small amounts of osteoid matrix, were retained in the xenografts after treatment with standard neoadjuvant chemotherapy (Fig. 4H-J).

The pattern of expression of the angiogenesis biomarker CD31 was also maintained between the original tumors (Fig. 5A,C) and the tumor grafts across three passages (Fig. 5B,D). Similarly, the expression pattern of antigen Ki-67 was well retained between the original tumor (Fig. 6A,C) and the corresponding xenograft at passage 2 (Fig. 6B,D).

To investigate the contribution of mouse stroma to tumor grafts, we performed staining for anti-human nuclear lamin A/C (Fig. 7). Immunostaining revealed that a portion of the components of the human-derived stroma was lost after engraftment as indicated by an overall higher proportion of human tumor cells within the grafts (Fig. 7A). Moreover, the contributions of murine stroma to tumor grafts were represented mostly by unstained mouse-derived endothelial cells forming the tumor vasculature (Fig. 7B,C).

The associations between positive or negative engraftment and demographic and clinicopathological

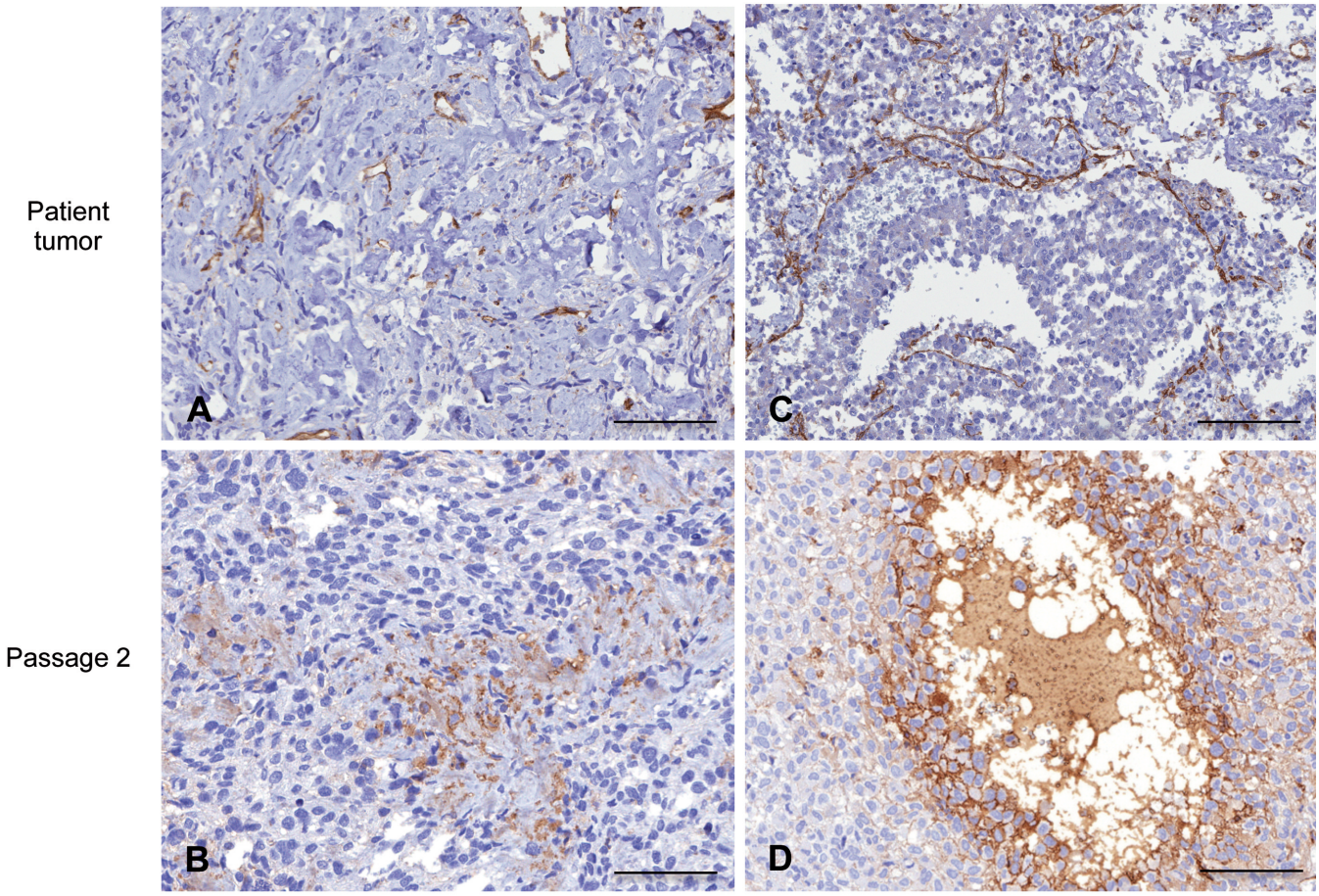


Fig. 5. Immunohistochemical staining for CD31 in representative histological specimens of primary osteosarcoma and tumor grafts. **A.** Conventional central osteosarcoma. **B.** Xenograft retained the biomarker expression pattern consistent with the original tumor **(A)**. **C.** Telangiectatic osteosarcoma. **D.** Note that antibody staining for CD31 identified characteristic vascular networks in the original tumor **(C)** was preserved in the tumor graft at passage 2. Scale bars: A, B, D, 100 µm; C, 200 µm.

factors are shown in Tables 1 and 2. Features such as patient's age and gender were not significantly associated with engraftment status. The engraftment efficiency of samples obtained after chemotherapy was significantly higher than that of samples obtained before chemotherapy (p=0.02).

Regardless of the absence of significant difference in primary tumor Enneking stage between engrafters and non-engrafters (p=0.07), the primary lesions of all engrafters were classified as Enneking stages IIB (n=7) and III (n=8) (high grade tumors). No specimen from primary tumors graded as Enneking stage I (n=2) (low grade) or IIA (n=2) (high grade but intracompartmental) produced a PDX. Also, tumor volume did not affect tumor engraftment (0=0.33). Patients with metastases at the time of diagnosis (n=10) had a significantly higher successful PDX engraftment (8 out of 10, p=0.003) compared to patients with localized disease at diagnosis (7 out of 27). The primary tumor specimens obtained from wide surgical resection gave rise to PDXs with a significantly higher efficiency than those obtained by core needle biopsy (p=0.008). The source of the samples of the tumors that successfully engrafted was predominantly from surgical specimens (10 out of 15) while most specimens obtained from biopsies (17 out of 22) failed to yield PDXs. In addition, PDX formation was not associated with local relapses (p=0.22) (Table 1).

Analysis of histopathological features of patient tumors demonstrated that the extent of necrosis induced by chemotherapy, perineural and/or lymphovascular invasion by tumor cells, and nuclear pleomorphism were not significantly associated with tumor engraftment. Also, no significant difference was observed in engraftment efficiency between histological subtype of osteosarcoma and primary tumor location (Table 2).

Table 1. Demographic and clinical findings of 37 patients with osteosarcoma by primary tumor engraftment and PDX formation.

Variable	Tumor engraftment and PDX formation n (%)		P-value*
	Negative (n=22)	Positive (n=15)	
Demographic data			
Male	12 (54.5)	12 (80.0)	0.11
Female	10 (45.5)	3 (20.0)	
Age, median (IQR)	18 (18)	18 (18)	0.73**
Neoadjuvant chemotherapy			
No	17 (77.3)	6 (40.0)	0.022
Yes	5 (22.7)	9 (60.0)	
Enneking staging (n=33)			
I A	0 (0.0)	0 (0.0)	
I B	2 (11.1)	0 (0.0)	
II A	2 (11.1)	0 (0.0)	0.07
II B	11 (61.1)	7 (46.7)	
III	3 (16.7)	8 (53.3)	
Tumor volume, $cm^{3\#}$ (n=36)			
≤999	16 (72.7)	8 (57.1)	0.33
≥1000	6 (27.3)	6 (42.9)	
Metastatic disease at diagnosis			
No	20 (90.9)	7 (46.7)	0.003
Yes	2 (9.1)	8 (53.3)	
Source of tumor tissue sample			
Core needle biopsy	17 (77.3)	5 (33.3)	0.008
Surgery	5 (22.7)	10 (66.7)	
Local relapses (n=27)			
No	16 (84.2)	5 (62.5)	0.22
Yes	3 (15.8)	3 (37.5)	

#: Tumor volume at the time of surgery was calculated in images originated from computed tomography in Digital Imaging and Communication in Medicine DICOM format version 3.0.0. Measurements were obtained using the crosshair tool and selecting the largest diameter of the images of the lesions in axial, coronal and sagittal reconstructed views. *: Chi-square or Fisher's exact text and **: Mann-Whitney test. PDX, Patient-derived xenograft; IQR, interquartile range.

Table 2. Clinicopathological characteristics of 37 patients with osteosarcoma by primary tumor engraftment and PDX formation.

Variable	Tumor engraftment and PDX formation n (%)		P-value*
	Negative (n=22)	Positive (n=15)	
Histologic variants			
Central high-grade conventional	19 (86.4)	12 (80.0)	
Central low-grade	1 (4.5)	0 (0)	
Telangiectatic	0 (0)	1 (6.7)	0.17
Small cell	0 (0)	2 (13.3)	
Parosteal	2 (9.1)	0 (0)	
Tumor viability after chemotherapy			
0-9%	4 (28.6)	1 (9.1)	
10-49%	2 (14.3)	0 (0)	0.16
≥50%	8 (57.1)	10 (90.9)	
Not available	8	4	
Tumor location			
Femur	16 (72.7)	8 (53.3)	
Tibia	5 (22.7)	3 (20.0)	0.26
Fibula	1 (4.6)	3 (20.0)	
Talus	0 (0.0)	1 (6.7)	
Lymphovascular invasion#			
No	15 (83.3)	10 (76.9)	0.66
Yes	3 (16.7)	3 (23.1)	
Not available	4	2	
Perineural invasion#			
No	18 (100)	12 (92.3)	0.23
Yes	0 (0.0)	1 (7.7)	
Not available	4	2	
Nuclear pleomorphism§			
Slight	7 (31.8)	1 (6.7)	
Moderate	8 (36.4)	8 (53.3)	0.19
High	7 (31.8)	6 (40.0)	

#: Lymphovascular and perineural invasion were considered present when tumor cells were identified respectively within an endothelial-lined space or the space surrounding a nerve. §: Nuclear pleomorphism was evaluated in the areas with most intense nuclear atypia and graded as slight when the nuclei displayed minimal variability in size and shape; moderate when the variation in size and shape was intermediate and high for marked nuclear variation in size and shape. *: Chi-square or Fisher's exact test. PDX, Patient-derived xenograft.

Discussion

Translational cancer models that recapitulate with high fidelity the intricate microenvironment of osteosarcomas are an important platform to assess novel targeted therapies and to guide clinical decisions in individualized medicine. However, given the low frequency of musculoskeletal malignancies, the number of sarcoma PDX models is relatively small compared to models in other tumor types, particularly carcinomas (Julien et al., 2012; De Rose et al., 2013; Zhang et al., 2013; Ricci et al., 2014; Depreeuw et al., 2015; Pergolini et al., 2017). In this setting, the amplification of the existing library of PDX tumor models of bone sarcomas (Blattmann et al., 2015; Stewart et al., 2017; Zhang et al., 2017; Lu et al., 2018; Meohas et al., 2018; Rainusso et al., 2018; Nanni et al., 2019) will allow substantial advances in basic and clinical cancer research.

We have successfully established 15 PDXs from a single type of bone sarcoma with an overall engraftment efficiency of 40.54% (15/37). Similar results were reported recently with xenografts established with 36% of the parental primary tumor (Nanni et al., 2019). In the literature, an overall engraftment efficiency ranging from 20% (Bruheim et al., 2004) to 49% (Stewart et al., 2017) only for osteosarcoma and from 45% (Stewart et al., 2017) to 51% (Rainusso et al., 2018) for bone sarcomas in general has been reported.

In our study, the mice were observed for 7 months before the final scoring of a positive or a negative engraftment was determined. We noticed that the latency period and the rate of PDX growth were highly variable from patient to patient. After implantation of primary tumor samples in mice, some xenografts became palpable within only a few weeks, while other tumors took up to 36 weeks to generate a palpable graft. Similarly, the median PDX growth period ranged from 52-367 days (median 173 days). Variation in the growth dynamics of osteosarcoma PDX tumors has also been reported by other groups (Stewart et al., 2017; Rainusso et al., 2018; Nanni et al., 2019) and may suggest that fast-growing tumors may represent a more aggressive disease in which the biological mechanisms that allow these tumors to adapt and grow in a new environment

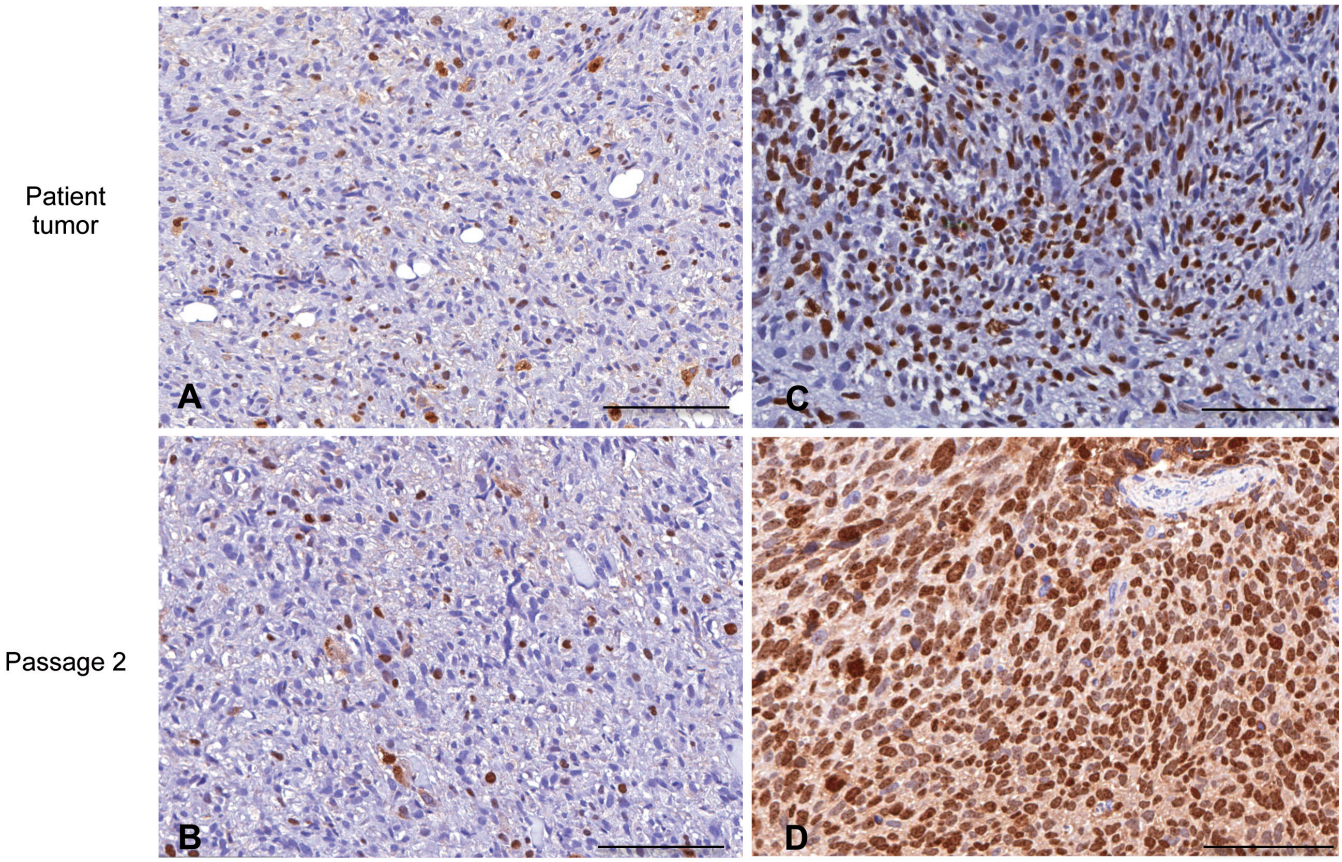


Fig. 6. Immunohistochemical staining for Ki-67 in representative histological specimens of primary osteosarcoma and tumor grafts. **A.** Conventional central osteosarcoma. **B.** The pattern of expression of Ki-67 was well maintained between the original tumor **(A)** and the corresponding xenograft at passage 2. **C.** Small cell osteosarcoma. **D.** The biomarker expression pattern resembled the original tumor from which it was derived **(C)**. Scale bars: A-C, 100 μm; D, 200 μm.

are somehow facilitated.

In general, PDX tumor models accurately preserve the morphological features of the original tumor (Julien et al., 2012; De Rose et al., 2013; Ricci et al., 2014; Izumchenko et al., 2017; Cornillie et al., 2019; Nanni et al., 2019). In the present study we confirmed that the morphological characteristics of the parental tumors were well preserved in the PDX models after up to three passages in the nude mice. The histopathological fidelity between the patient tumor and their respective PDX tumors was confirmed by the maintenance in the grafts of histological hallmarks of the osteosarcoma variant, mostly the pattern of neoplastic osteoid/bone matrix deposition and tumor anaplasia. Another important feature of the PDXs described herein is the retention of the proliferative profile between initial tumors and xenografted tumors at P2, as assessed by Ki-67 staining. The immunohistochemical concordance with the tumor of origin indicated biological consistency of the xenograft with the primary tumor and stability of the preclinical model after serial passage in mice (De Rose et al., 2013; Depreeuw et al., 2015; Stewart et al., 2017; Nanni et al., 2019).

Of particular interest are our results for anti-human nuclear lamin A/C with respect to the relative contributions of human-derived and mouse-derived stroma to the tumor grafts. Although the global histological architecture of the graft was preserved, we observed that human tumor cells were closely packed, suggesting a process of stromal retraction after engraftment. Moreover, newly formed capillaries lined by mouse-derived endothelial cells represented tumor vasculature. The overall replacement of the human vascular network from the original tumor with capillaries from the host mouse might impose limitations on the current model. As a result, the grafts might display an increased tendency to necrotize and with a constraint to growth due to poor and insufficient vascularization, which will be independent of the biological aggressiveness of the tumor cells. To investigate the role of necrosis as a limiting factor for the growth of breast cancer PDX, De Rose et al. (2013) co-implanted established tumor grafts with primary human mesenchymal stem cells (MSCs). They found that although MSCs did not directly form blood vessels within the graft, co-engraftment of MSCs with breast cancers PDXs facilitated angiogenesis, reduced necrosis, and increased tumor growth.

In this study we also had the opportunity to generate a PDX derived from the same patient before and after exposure to cytotoxic chemotherapy. The post-chemotherapy xenografted tumor matched with that obtained prior to therapy and both retained the cellular features of the histologic variant of the patient tumor to a similar degree. The fact that the characteristics of the primary tumor remained unchanged after chemotherapy makes PDX models a unique system to investigate the mechanisms of chemo-resistance and to assess the efficacy of anticancer agents. In a previous study,

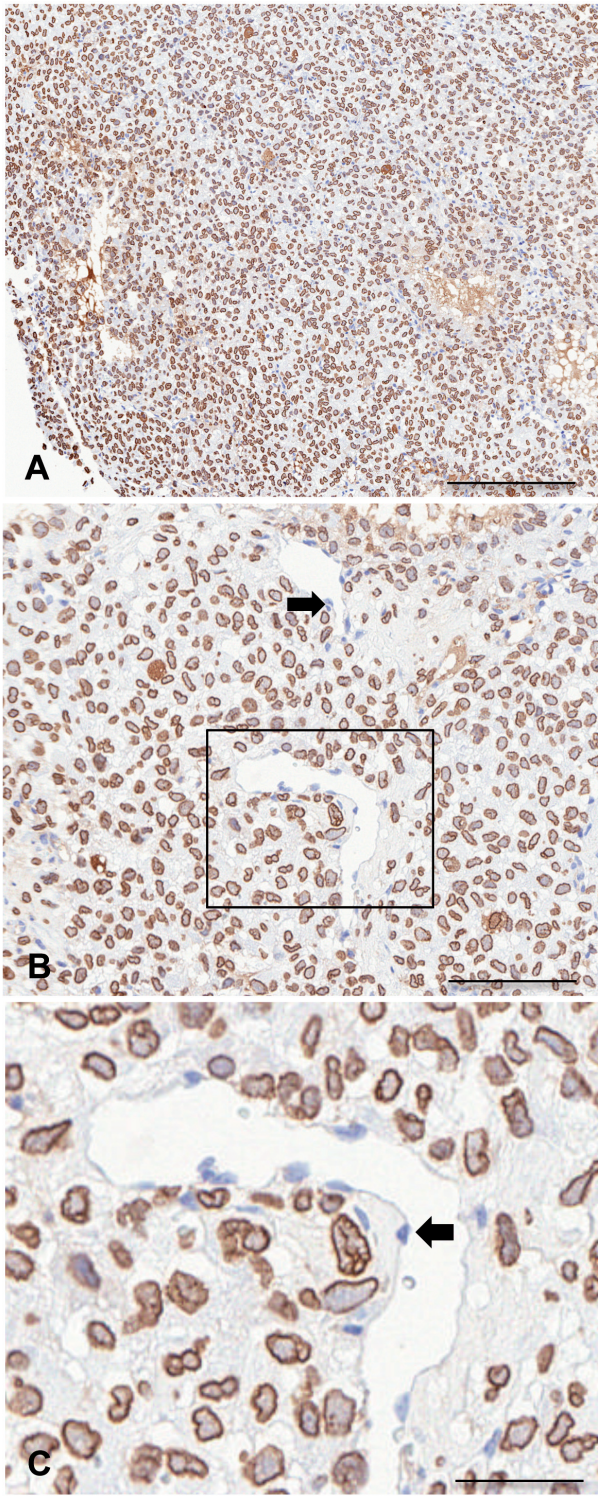


Fig. 7. Representative immunostaining with antibody specific for anti-human Lamin A/C. **A.** Tumor grafts at passage 2 were positive for human-specific Lamin staining detected in the nuclear membrane of tumor cells. **B.** The contribution of murine cells to tumor grafts was represented mostly by unstained (negative for human Lamin A/C) mouse-derived endothelial cells that formed the tumor vasculature (arrows). **C.** Higher magnification from vessel displayed in **(B)**. Scale bars: A, 50 µm; B, 100 µm; C, 200 µm.

Izumchenko et al. (2017) demonstrated that PDX models for several types of solid tumors faithfully conserved genetic patterns of the primary tumors and reflected patients' clinical outcomes, even after several additional cycles of therapy.

There is a paucity of studies that have investigated the relationship between successful tumor engraftment in a PDX model and clinicopathological features in mesenchymal malignancies (Bruheim et al., 2004). To our knowledge, there is no specific information available about the association of pathological factors with PDX models generated in a series including only osteosarcoma patients.

In our study, we found that the PDX take rate was higher in post-chemotherapy surgical samples. It is noteworthy that in osteosarcoma patients, wide surgical resection is available almost invariably after neoadjuvant chemotherapy. Considering that only a small portion of the patient tumor will be implanted, for successful PDX generation we consider it to be of utmost importance to direct tumor sampling based on gross macroscopic criteria. Important selection criteria include avoidance of areas of necrosis and extensive hemorrhage as well as sampling from representative regions of the tumor. Indeed, in the present study we have shown the feasibility of generating a PDX from a patient with less than 10% of viable post-chemotherapy residual tissue remaining. Thus, we agree with others (Rainusso et al., 2018) that a multidisciplinary team approach, including experienced pathologists, is critical to provide adequate tumor samples for successful PDX generation. Also, the higher take rate for samples obtained after chemotherapy could be explained by a natural selection by the chemotherapy in favor of the most aggressive tumor clones with greater growth and survival potential.

To our knowledge, this is the first report to compare the engraftment rate when transplanting osteosarcoma samples from surgical specimens and diagnostic biopsies. According to Stewart et al. (2017) and Rainusso et al. (2018), samples obtained by needle biopsies can provide adequate amounts of tumor tissue to establish osteosarcoma PDXs. Recently, Cornillie et al. (2019) reported no significant differences in the success rate between surgical specimens and diagnostic biopsy samples from patients with soft tissue sarcomas. However, in the present study, we were not able to replicate these results since our rates of successful engraftment were lower for samples obtained from core needle biopsies (22.72% versus 66.67% for surgical samples). This finding can be explained by: (1) an increased chance to transplant to the mice necrotic tissue only since osteosarcomas are almost invariably associated with extensive areas of necrosis; and (2) in samples randomly obtained through biopsy the smaller volume of tumor tissue does not allow selecting the fragment to be transplanted guided by well-defined gross examination criteria to identify tumor tissue. As a strategy to help to establish the biological factors contributing to positive engraftment rates, we validated by histological assessment all implanted tumor fragments as representative of the parental tumor.

Consistent with previous reports for other cancer types (Garrido-Laguna et al., 2011; De Rose et al., 2013), we found that more aggressive tumors, including those with metastatic disease at presentation, have a higher efficiency to generate PDXs. Also, despite the absence of a statistically significant difference in primary tumor Enneking stage between engrafters and non-engrafters, tumor engraftment and growth was observed in 8 out of 10 patients classified as Enneking Stage III (tumor with distant metastasis) suggesting that the take rate is higher in higher-grade disease. However, clinical markers of more aggressive disease such as clinical staging and tumor grade, tumor size at the time of diagnosis, local relapses as well as the histologic variant were not significantly associated with positive engraftment of the tumor tissue in the mice.

Subcutaneous PDX models, as with other translational oncologic models, have well recognized limitations. Spontaneous metastasis mimicking the progression of the human disease is described only in association with orthotopic models (Crnalic et al., 1997). Another drawback of the current model is the immunodeficient background of the mice enhancing or reducing the efficiency of tumor engraftment and the human-derived stroma substitution, which ultimately will change the tumor microenvironment and the genomic profiles of PDX (Ben-David et al., 2017). In this regard, the co-engraftment of immortalized human stromal cells was shown to support tumor angiogenesis and improve tumor growth after engraftment of human breast cancer (De Rose et al., 2013).

We consider the sample size to be an additional limitation of our study. Although we collected 37 samples of a rare malignancy, we fear that these samples may not be representative of the genetic heterogeneity found in and among patients with osteosarcoma (Martin el al., 2012; Mirabello et al., 2020). This heterogeneity can result in different biological behaviors of the tumor that will ultimately influence the clinical evolution of the patient and the engraftment rates. Moreover, larger series of osteosarcoma preclinical models are needed to confirm our findings regarding the association between clinicopathological variables and positive engraftment.

In conclusion, our study showed that the osteosarcoma PDX model described here reliably recapitulated the morphological aspects of the human disease after serial passage in nude mice. The similarities with original tumor specimens are indirect evidence that the tumors implanted into mice sustain the ability to interact with supporting stromal cells and, therefore provide a promising scenario to address several unanswered issues in clinical oncology. Furthermore, more aggressive forms of osteosarcoma, including those with metastatic disease at presentation, have a higher efficiency to generate PDXs.

Acknowledgements. This study was supported by the Brazilian Ministry of Health (National Institute of Traumatology and Orthopedics).
Disclosure of Potential Conflicts of Interest. No potential conflicts of interest were disclosed.

References

Ben-David U., Ha G., Tseng Y., Greenwald N.F., Oh C., Shih J., McFarland J.M., Wong B., Boehm J.S., Beroukhim R. and Golub T.R. (2017). Patient-derived xenografts undergo mouse-specific tumor evolution. Nat. Genet. 49, 1567-1575.

Bielack S.S. and Bernstein M.L. (2005). Osteosarcoma. In: Cancer in Children: clinical management. 5th ed. Voute P.A., Barrett A., Stevens M.C.G. and Caron H.N. (eds). Oxford University Press. Oxford. pp 280-300.

Bielack S.S., Kempf-Bielack B., Delling G., Exner G.U., Flege S., Helmke K., Kotz R., Salzer-Kuntschik M., Werner M., Winkelmann W., Zoubek A., Jürgens H. and Winkler K. (2002). Prognostic factors in high-grade osteosarcoma of the extremities or trunk: an analysis of 1,702 patients treated on neoadjuvant cooperative osteosarcoma study group protocols. J. Clin. Oncol. 20, 776-790.

Blattmann C., Thiemann M., Stenzinger A., Roth E.K., Dittmar A., Witt H., Lehner B., Renker E., Jugold M., Eichwald V., Weichert W., Huber P.E. and Kulozik P.E. (2015). Establishment of a patient-derived orthotopic osteosarcoma mouse model. J. Transl. Med. 13, 136.

Bruheim S., Bruland O.S., Breistol K., Maelandsmo G.M. and Fodstad O. (2004). Human osteosarcoma xenografts and their sensitivity to chemotherapy. Pathol. Oncol. Res. 10, 133-141.

Cornillie J., Wozniak A., Li H., Wang Y., Boeckx B., Gebreyohannes Y.K., Wellens J., Vanleeuw U., Hompes D., Stas M., Sinnaeve F., Wafa H., Lambrechts D., Debiec-Rychter M., Sciot R. and Schöffski P. (2019). Establishment and characterization of histologically and molecularly stable soft tissue sarcoma xenograft models for biological studies and preclinical drug testing. Mol. Cancer Ther. 18, 1168-1178.

Crnalic S., Hakansson I., Boquist L., Lofvenberg R. and Brostrom L.A. (1997). A novel spontaneous metastasis model of human osteosarcoma developed using orthotopic transplantation of intact tumor tissue into tibia of nude mice. Clin. Exp. Metastasis 15, 164-172.

Daniel V.C., Marchionni L., Hierman J.S., Rhodes J.T., Devereux W.L., Rudin C.M., Yung R., Parmigiani G., Dorsch M., Peacock C.D. and Watkins D.N. (2009). A primary xenograft model of small-cell lung cancer reveals irreversible changes in gene expression imposed by culture *in vitro*. Cancer Res. 69, 3364-3373.

De Rose Y.S., Wang G., Lin Y., Bernard P.S., Buys S.S., Ebbert M.T.W, Factor R., Matsen C., Milash B.A., Nelson E., Neumayer L., Randall R.L., Stijleman I.J., Welm B.E. and Welm A.L. (2013). Tumor grafts derived from women with breast cancer authentically reflect tumor pathology, growth, metastasis and disease outcomes. Nat. Med. 17, 1514-1520.

Depreeuw J., Hermans E., Schrauwen S., Annibali D., Coenegrachts L., Thomas D., Luyckx M., Gutierrez-Roelens I., Debruyne D., Konings K., Moerman P., Vergote I., Lambrechts D. and Amant F. (2015). Characterization of patient-derived tumor xenograft models of endometrial cancer for preclinical evaluation of targeted therapies. Gynecol. Oncol. 139, 118-126.

Ding L., Ellis M.J., Li S., Larson D.E., Chen K., Wallis J.W., Harris C.C., McLellan M.D., Fulton R.S., Fulton L.L., Abbott R.M., Hoog J., Dooling D.J., Koboldt D.C., Schmidt H., Kalicki J., Zhang Q., Chen L., Lin L., Wendl M.C., McMichael J.F., Magrini V.J., Cook L., McGrath S.D., Vickery T.L., Appelbaum E., Deschryver K., Davies S., Guintoli T., Lin L., Crowder R., Tao Y., Snider J.E., Smith S.M., Dukes A.F., Sanderson G.E., Pohl C.S., Delehaunty K.D., Fronick C.C., Pape K.A., Reed J.S., Robinson J.S., Hodges J.S., Schierding W., Dees N.D., Shen D., Locke D.P., Wiechert M.E., Eldred J.M., Peck J.B., Oberkfell B.J., Lolofie J.T., Du F., Hawkins A.E., O'Laughlin M.D., Bernard K.E., Cunningham M., Elliott G., Mason M.D., Thompson D.M. Jr., Ivanovich J.L., Goodfellow P.J., Perou C.M., Weinstock G.M., Aft R., Watson M., Ley T.J., Wilson R.K. and Mardis E.R. (2010). Genome remodelling in a basal-like breast cancer metastasis and xenograft. Nature 464, 999-1005.

Garber K. (2009). From human to mouse and back: "Tumorgraft'' models surge in popularity. J. Natl. Cancer Inst. 101, 6-8.

Garrido-Laguna I., Uson M., Rajeshkumar N.V., Tan A.C., de Oliveira E., Karikari C., Villaroel M.C., Salomon A., Taylor G., Sharma R., Hruban R.H., Maitra A., Laheru D., Rubio-Viqueira B., Jimeno A. and Hidalgo M. (2011). Tumor engraftment in nude mice and enrichment in stroma-related gene pathways predict poor survival and resistance to gemcitabine in patients with pancreatic cancer. Clin. Cancer Res. 17, 5793-5800.

Isakoff M.S., Bielack S.S., Meltzer P. and Gorlick R. (2015). Osteosarcoma: current treatment and a collaborative pathway to success. J. Clin. Oncol. 33, 3029-3035.

Izumchenko E., Paz K., Ciznadija D., Sloma I., Katz A., Vasquez-Dunddel D., Ben-Zvi I., Stebbing J., McGuire W., Harris W., Maki R., Gaya A., Bedi A., Zacharoulis S., Ravi R., Wexler L.H., Hoque M.O., Rodriguez-Galindo C., Pass H., Peled N., Davies A., Morris R., Hidalgo M. and Sidransky D. (2017). Patient-derived xenografts effectively capture responses to oncology therapy in a heterogeneous cohort of patients with solid tumors. Ann. Oncol. 28, 2595-2605.

Jawad M.U. and Scully S.P. (2010). In brief: Classifications in brief: Enneking classification: benign and malignant tumors of the musculoskeletal system. Clin. Orthop. Rel. Res. 468, 2000-2002.

John T., Kohler D., Pintilie M., Yanagawa N., Pham N.A., Li M., Panchal D., Hui F., Meng F., Shepherd F.A. and Tsao M.S. (2011). The ability to form primary tumor xenografts is predictive of increased risk of disease recurrence in early-stage non-small cell lung cancer. Clin. Cancer Res. 17, 134-141.

Joshua B., Kaplan M.J., Doweck I., Pai R., Weissman I.L., Prince M.E. and Ailles L.E. (2012). Frequency of cells expressing CD44, a head and neck cancer stem cell marker: correlation with tumor aggressiveness. Head Neck 34, 42-49.

Julien S., Merino-Trigo A., Lacroix L., Pocard M., Goéré D., Mariani P., Landron S., Bigot L., Nemati F., Dartigues P., Weiswald L.B., Lantuas D., Morgand L., Pham E., Gonin P., Dangles-Marie V., Job B., Dessen P., Bruno A., Pierré A., De Thé H., Soliman H., Nunes M., Lardier G., Calvet L., Demers B., Prévost G., Vrignaud P., Roman-Roman S., Duchamp O. and Berthet C. (2012). Characterization of a large panel of patient-derived tumor xenografts representing the clinical heterogeneity of human colorectal cancer. Clin. Cancer Res. 18, 5314-5328.

Kim M.P., Evans D.B., Wang H., Abbruzzese J.L., Fleming J.B. and Gallick G.E. (2009). Generation of orthotopic and heterotopic human

pancreatic cancer xenografts in immunodeficient mice. Nat. Protoc. 4, 1670-1680.

Kresse S.H., Meza-Zepeda L.A., Machado I., Llombart-Bosch A. and Myklebost O. (2012). Preclinical xenograft models of human sarcomas show nonrandom loss of aberrations. Cancer 118, 558-570.

Langdon S.P. (2012). Animal modeling of cancer pathology and studying tumor response to therapy. Curr. Drug Targets 13, 1535-1547.

Lu W., Chao T., Ruiqi C., Juan S. and Zhihong L. (2018). Patient-derived xenograft models in musculoskeletal malignancies. J. Transl. Med. 16, 107.

Martin J.W., Squire J.A. and Zielenska M. (2012). The genetics of osteosarcoma. Sarcoma 2012, 627254.

McAuliffe P.F., Evans K.W., Akcakanat A., Chen K., Zheng X., Zhao H., Eterovic A.K., Sangai T., Holder A.M., Sharma C., Chen H., Do K.A., Tarco E., Gagea M., Naff K.A., Sahin A., Multani A.S., Black D.M., Mittendorf E.A., Bedrosian I., Mills G.B., Gonzalez-Angulo A.M. and Meric-Bernstam F. (2015). Ability to generate patient-derived breast cancer xenografts is enhanced in chemoresistant disease and predicts poor patient outcomes. PLoS One 10, e0136851.

Meohas W., Granato R.A., Guimarães J.A.M., Dias R.B., Fortuna-Costa A. and Duarte M.E.L. (2018). Patient-derived xenografts as a preclinical model for bone sarcomas. Acta Ortop. Bras. 26, 98-102.

Mirabello L., Troisi R.J. and Savage S.A. (2009a). International osteosarcoma incidence patterns in children and adolescents, middle ages and elderly persons. Int. J. Cancer 125, 229-234.

Mirabello L., Troisi R.J. and Savage S.A. (2009b). Osteosarcoma incidence and survival rates from 1973 to 2004: data from the Surveillance, Epidemiology, and End Results Program. Cancer 115, 1531-1543.

Mirabello L., Zhu B., Koster R., Karlins E., Dean M., Yeager M., Gianferante M., Spector L.G., Morton L.M., Karyadi D., Robison L.L., Armstrong G.T., Bhatia S., Song L., Pankratz N., Pinheiro M., Gastier-Foster J.M., Gorlick R., de Toledo S.R.C., Petrilli A.S., Patino-Garcia A., Lecanda F., Gutierrez-Jimeno M., Serra M., Hattinger C., Picci P., Scotlandi K., Flanagan A.M., Tirabosco R., Amary M.F., Kurucu N., Ilhan I.E., Ballinger M.L., Thomas D.M., Barkauskas D.A., Mejia-Baltodano G., Valverde P., Hicks B.D., Zhu B., Wang M., Hutchinson A.A., Tucker M., Sampson J., Landi M.T., Freedman N.D., Gapstur S., Carter B., Hoover R.N., Chanock S.J. and Savage S.A. (2020). Frequency of pathogenic germline variants in cancer-susceptibility genes in patients with osteosarcoma. JAMA Oncol. 6, 724-734.

Monsma D.J., Monks N.R., Cherba D.M., Dylewski D., Eugster E., Jahn H., Srikanth S., Scott S.B., Richardson P.J., Everts R.E., Ishkin A., Nikolsky Y., Resau J.H., Sigler R., Nickoloff B.J. and Webb C.P. (2012). Genomic characterization of explant tumorgraft models derived from fresh patient tumor tissue. J. Transl. Med. 10, 125.

Nanni P., Landuzzi L., Manara M.C., Righi A., Nicoletti G., Cristalli C., Pasello M., Parra A., Carrabotta M., Ferracin M., Palladini A., Ianzano M.L., Giusti V., Ruzzi F., Magnani M., Donati D.M., Picci P., Lollini P.L. and Scotlandi K. (2019). Bone sarcoma patient-derived xenografts are faithful and stable preclinical models for molecular and therapeutic investigations. Sci. Rep. 9, 12174.

Noone A.M., Howlader N., Krapcho M., Miller D., Brest A., Yu M., Ruhl J., Tatalovich Z., Mariotto A., Lewis D.R., Chen H.S., Feuer E.J. and Cronin K.A. (2018). SEER cancer statistics review, 1975–2015. National Cancer Institute; Bethesda, MD: Based on November 2017 SEER data submission to the SEER web site, April 2018. Available from: URL: https://seer.cancer.gov/csr/1975_2015/. Accessed February 20, 2020.

Pergolini I., Morales-Oyarvide V., Mino-Kenudson M., Honselmann K.C., Rosenbaum M.W., Nahar S., Kem M., Ferrone C.R., Lillemoe K.D., Bardeesy N., Ryan D.P., Thayer S.P., Warshaw A.L., Fernández-Del Castillo C. and Liss A.S. (2017). Tumor engraftment in patient-derived xenografts of pancreatic ductal adenocarcinoma is associated with adverse clinicopathological features and poor survival. PLoS One 12, e0182855.

Press J.Z., Kenyon J.A., Xue H., Miller M.A., De Luca A., Miller D.M., Huntsman D.G., Gilks C.B., McAlpine J.N. and Wang Y.Z. (2008). Xenografts of primary human gynecological tumors grown under the renal capsule of NOD/SCID mice show genetic stability during serial transplantation and respond to cytotoxic chemotherapy. Gynecol. Oncol. 110, 256-264.

Rainusso N., Cleveland H., Hernandez J.A., Quintanilla N.M., Hicks J., Vasudevan S., Marco R.A.W., Allen-Rhoades W., Wang L.L. and Yustein J.T. (2018). Generation of patient-derived tumor xenografts from percutaneous tumor biopsies in children with bone sarcomas. Pediatr. Blood Cancer 66, e27579.

Ricci F., Bizzaro F., Cesca M., Guffanti F., Ganzinelli M., Decio A., Ghilardi C., Perego P., Fruscio R., Buda A., Milani R., Ostano P., Chiorino G., Bani M.R., Damia G. and Giavazzi R. (2014). Patient-derived ovarian tumor xenografts recapitulate human clinicopathology and genetic alterations. Cancer Res. 74, 6980-6990.

Siolas D. and Hannon G.J. (2013). Patient-derived tumor xenografts: transforming clinical samples into mouse models. Cancer Res. 73, 5315-5319.

Stewart E., Federico S.M., Chen X., Shelat A.A., Bradley C., Gordon B., Karlstrom A., Twaroq N.R., Clay M.R., Bahrami A., Freeman B.B. 3rd., Xu B., Zhou X., Wu J., Honnell V., Ocarz M., Blankenship K., Dapper J., Mardis E.R., Wilson R.K., Downing J., Zhang J., Easton J., Pappo A. and Dyer M.A. (2017). Orthotopic patient-derived xenografts of paediatric solid tumours. Nature 549, 96-100.

Tentler J.J., Tan A.C., Weekes C.D., Jimeno A., Leong S., Pitts T.M., Arcaroli J.J., Messersmith W.A. and Eckhardt S.G. (2012). Patient-derived tumour xenografts as models for oncology drug development. Nat. Rev. Clin. Oncol. 9, 338-350.

Zhang X., Zhang J., Li M., Huang X., Yang X., Zhong W., Xie L., Zhang L., Zhou M., Gavine P., Su X., Zheng L., Zhu G., Zhan P., Ji Q. and Wu Y.L. (2013). Establishment of patient-derived non-small cell lung cancer xenograft models with genetic aberrations within EGFR, KRAS and FGFR-1: useful tools for preclinical studies of targeted therapies. J. Transl. Med. 11, 168.

Zhang T., Li J., Yin F., Bin B., Wang Z., Xu J., Wang H., Zuo D., Wang G., Hua Y. and Cai Z. (2017). Toosendanin demonstrates promising antitumor efficacy in osteosarcoma by targeting STAT 3. Oncogene 36, 6627-6639.

Accepted September 23, 2020